30th EPS Conference on Contr. Fusion and Plasma Phys., St. Petersburg, 7-11 July 2003 ECA Vol. 27A, P-1.129

Active edge localized mode (ELM) frequency control with pellets

P.T. Lang*, A. Kallenbach, L. Fattorini[1], L.D. Horton, J. Neuhauser, H. Urano, ASDEX Upgrade Team

Max-Planck-Institut für Plasmaphysik, EURATOM Association, Boltzmannstr. 2, 85748 Garching, Germany
[1] *Centro de Fusão Nuclear, Associacão EURATOM/IST, Instituto Superior Técnico, 1046-001 Lisboa, Portugal*
* *Corresponding author; e-mail: ptl@ipp.mpg.de*

1. Introduction

The occurrence of edge localized mode (ELM) activity seems to be a common feature in magnetically confined plasmas when accessing high confinement regimes. ELM events, characterized by a transient confinement collapse at the plasma edge, result in strong energy and particle bursts from plasma. These bursts can form a hazard for in-vessel components. Hence, a technique would be desirable to achieve external control of the ELM frequency. Pellets are already known to trigger ELMs when injected during type-I ELMy H-mode phases [1]. Here, we report on a successful experimental approach at ASDEX Upgrade [2] to increase the ELM frequency and mitigate losses per ELM in type-I regime plasma discharges by repetitive injection of small pellets.

2. Experimental setup

For the study presented, we choose a configuration with $I_P = 1MA$, $B_t = -2.7T$, $q_{95} = 4.9$, $\kappa = 1.6$, $\delta^u = 0.12$ and $\delta^l = 0.37$. The applied neutral beam injection (NBI) heating of 3.5 MW, just above the L-H transition power threshold, results in stable and robust operation in the type-I ELM regime with rather low natural ELM frequency as desired for demonstration of active ELM frequency control with the existing pellet injector. Depending on the actual wall conditions, these discharges developed a natural ELM frequency in the range 20 to 40 Hz for no or modest external gas puffing, with the ELM frequency a bit higher and the ELM size accordingly smaller in the latter case.
The pellet injector is based on a centrifuge pellet accelerator equipped with a storage cryostat capable of delivering up to 120 pellets. In order to deliver pellets sufficiently small to prevent too strong refueling at the desired high repetition rate, it was necessary to further reduce the nominally smallest pellet size from the existing hardware originally designed for deep pellet fueling. This was achieved by exploiting the special features of the "looping-II" set-up [3]. Nominal $(1.4mm)^3$ cubic pellets injected through the 17 m long guiding tube at a speed of 1 km/s are continuously reduced in size by transfer losses to about 1×10^{19} D-atoms entering the plasma, while keeping the delivery reliability still beyond 0.9. Applying this injector setting and omitting pellets on purpose, pellet repetition frequencies $f_P = \frac{250}{n}, n = 3, 4, 5...$ can be obtained.

3. Results

3.1. Controlling the ELM frequency

The basic idea behind ELM control is to choose the parameters in such a way that spontaneous ELMs are avoided, i.e. only ELMs initiated by a pellet appear. This requires that pellets can trigger ELMs reliably and, in addition, that the pellet frequency is sufficiently high. In fact, it has been found that every pellet injected during such type-I ELM phases triggered an ELM, with the minimum required pellet size obviously well

below 1×10^{19} D-atoms. With respect to the second condition, it has been found that $f_{Pel} > 1.5 \times f^0_{ELM}$ is required.

In this way, full ELM control is achieved with the desired increase of f_{ELM} by increasing f_{Pel} as seen in fig. 1. Here, the ELM frequency (averaged over 0.2 s) and the pellet controlled ELM fraction $c \equiv \frac{f_{ELM}}{f_{Pel}}$ are plotted as obtained in a discharge series performing a f_{Pel} scan. In these discharges, f^0_{ELM} was about 30 Hz. For the lowest f_{Pel} of 20.8 Hz, an enhancement of f_{ELM} takes place during the pellet phase (indicated as shaded area), while c reaches 0.5 only. At $f_{Pel} = 41.7$ Hz slightly above f^0_{ELM}, c is already close to unity. Full external ELM control and essentially c = 1 is established at the highest frequencies. f_{ELM} is equal to the selected value for 62.5 Hz while for the maximum setting of 83.3 Hz a few missing pellets reduce the real frequency to about 70 Hz. The scan proves that full external ELM frequency control is possible at least in the frequency range of about $1.5 - 3 \times f^0_{ELM}$, with the upper boundary only given by technical limitations.

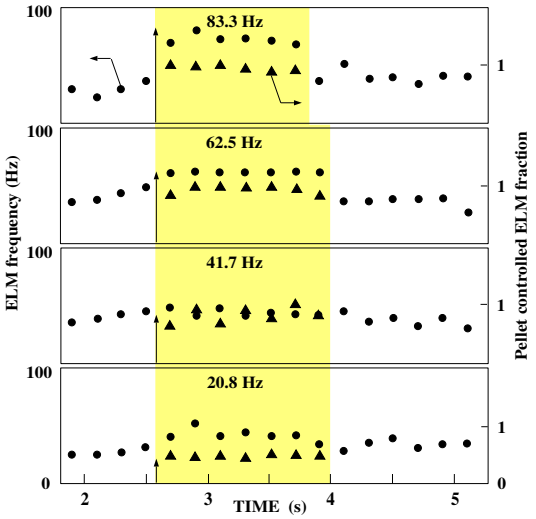

Figure 1: Pellet frequency scan. Increasing f_{Pel} during pellet phase (shaded area) results in f_{ELM} increase beyond f^0_{ELM}. A pellet controlled ELM fraction $c \equiv \frac{f_{ELM}}{f_{Pel}}$ approaching unity indicates full ELM control.

3.2. Impact on the plasma performance

The external enhancement of f_{ELM} causes confinement reduction. This effect, observed when increasing f^0_{ELM} by increasing the gas puff rate or the heating power, takes place also for external ELM frequency enhancement. However, the observed confinement reduction is quite modest, as shown in figure 2. The left part shows the temporal evolution of the discharge with a requested $f_{ELM} = 83.3$ Hz phase. Before and after the pellet sequence, reference phases were performed, the latter one including an additional gas puff $\Gamma_{gas} = 7 \times 10^{21}/s$, almost equal the pellet particle flux. As can be seen, the additional gas puff causes a density enhancement like the pellet imposed one while causing only a weak ELM frequency rise and confinement reduction with respect to its unpuffed counterpart. For all three phases the key parameters f_{ELM}, W_{MHD} and $\bar{n}_e$ are extracted during quiescent phases. All data obtained from the pellet frequency scan are given in the right part of figure 2, where $\bar{n}_e$ and W_{MHD} data are plotted versus f_{ELM}. Squares and triangles represent for the $\Gamma = 0$ and the gas puff reference phases, respectively; circles indicate pellet phases. Again, the slight density increase and energy decrease imposed by the gas puff as well as the mild refueling constraint of pellet injection becomes visible. However, most important, there is only a quite modest confinement decrease with pellet enhanced f_{ELM}, $W_{MHD} \sim f^{-0.16}_{ELM}$, much weaker than predicted from the empirical scaling derived for AUG and JET type-I ELMy mode plasmas, yielding $W_{MHD} \sim f^{-0.6}_{ELM}$ [4]. This pellet imposed confinement reduction, e.g. about $\frac{dW}{W_0} \approx 0.10$ for $f_{Pel} = 68Hz$, might be caused mostly by convective losses due to enhanced edge particle throughput: A flux of 7×10^{21} D atoms with a temperature of about 1 keV would result in an additional loss power of about 0.34 MW $\approx 0.096 \times P_{heat}$, consistent with the observed energy reduction. Thus, further reduction of the energy loss seems possible by a reduction of the pellet size.

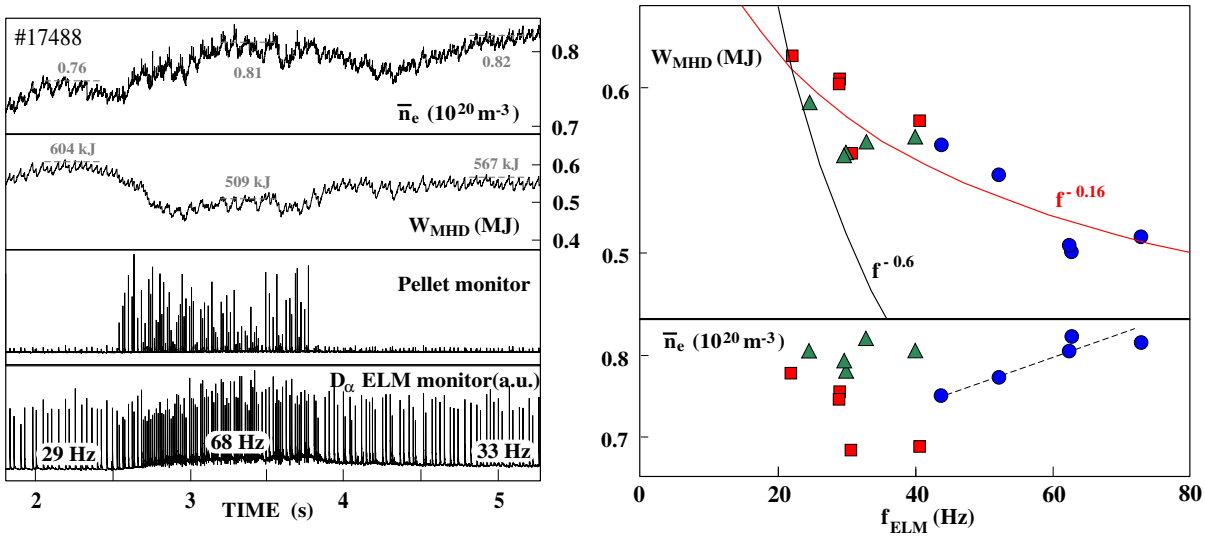

Figure 2: Left: Density, energy and ELM frequency evolution during phases without pellets and external puff, with small pellets and no puff, and with external gas puff only. Right: Data obtained from no gas (squares), gas puffed (triangles) and pellet phases (circles) versus f_{ELM}. Increasing f_{Pel} imposes slight refueling and confinement degradation. A fit to data unveils $W_{MHD} \sim f_{ELM}^{-0.16}$ much less pronounced than $\sim f_{ELM}^{-0.6}$ predicted for natural ELMs.

3.3. ELM features

On important motivation for external ELM control was the hope to mitigate the energy loss and maximum power flux per ELM and prevent potential hazards for in-vessel components. Indeed, this desired effect could be verified. All ELMs detected in this investigation - both in pellet and reference phases - fit well into a dataset derived for ASDEX Upgrade and JET data [6]. This scaling unveils that about 20% of the heating power is expelled by ELMs. Since, for pellet triggered ELMs, this is not on the expense of a strong confinement degradation, the energy loss per ELM reduces with increasing f_{ELM}. With a virtually unchanged ELM duration, also the power flux is mitigated. This is shown in fig.3, where a typical natural and a pellet triggered ELM are compared in a case where pellets raised f_{ELM}^0 by more than a factor 2. Whereas the pellet triggered ELM obviously still shows type-I features - as indicated by Mirnov coil and D_α radiation signal - the energy loss and the maximum power flux into the divertor is mitigated. Energy and power flux reduction takes place for both the inner and the outer divertor leg. The release is more pronounced for the outer divertor, further increasing the in/out power flux asymmetry.

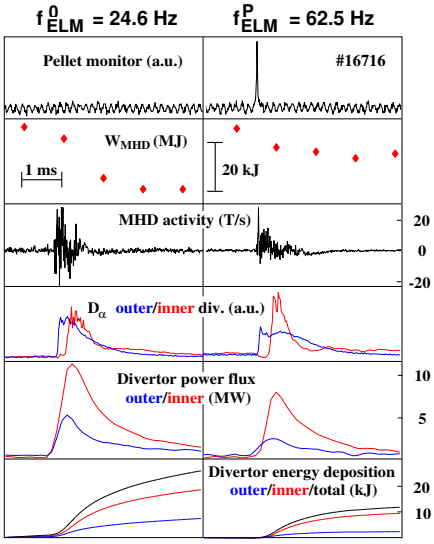

Figure 3: Comparison of natural and pellet triggered ELM. The pellet induced ELM still shows typical type-I features, but causes reduction in energy loss and mitigates divertor power flux and energy deposition

3.4. Application of ELM control in a high performance radiative feedback scenario

A high performance scenario for simultaneous feedback control of the divertor neutral flux (separatrix density, pumping) and the divertor temperature using impurity injection controlled by argon puffing has been developed at ASDEX Upgrade [5]. The 'effective' divertor temperature is obtained from online measurements of the thermoelectric currents flowing between the inner and outer divertor [6], which are a measure for the difference of the divertor temperatures. The thermoelectric $T_{e,eff}$ was found to be a sensitive measure for divertor conditions of plasmas with good H-mode confinement. During the investigation of radiative feedback scenarios in the type-I ELMy regime, a radiative run-away situation is often observed in the vicinity of the H-L threshold: Radiation rise in between type-I ELMs leads to a further delay of the next ELM, with ongoing radiation increase until a short H-L transition occurs. This is quickly cured by the feedback, but does not lead to stationary conditions.

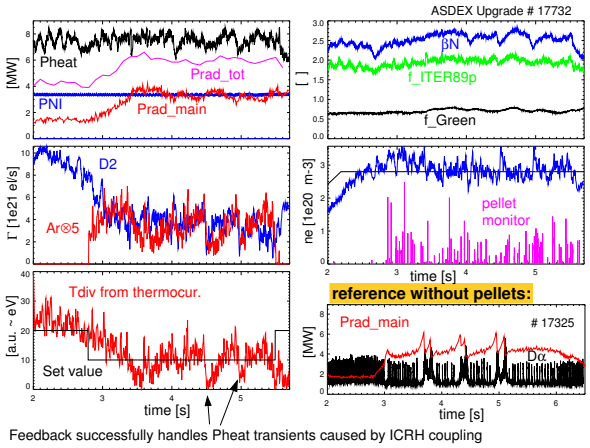

Figure 4: Discharge with feedback of the divertor temperature using Ar puffing. The divertor neutral D flux is controlled via an ionization gauge measurement and D puffing. Small pellet injection with 40 Hz ensures a corresponding minimum ELM frequency. Without the pellet ELM trigger, longer ELM-free periods develop, which lead to increased Ar radiation further delaying te next ELM with a possible H-L transition (see lower right picture).

Adding external ELM triggering by small pellets, the radiative run-away situation is avoided. Figure 4 shows an example for a discharge with simultaneous divertor neutral flux and temperature feedback combined with ELM frequency control. These discharges combine high β_N, H-factor and Greenwald fraction and retain low central tungsten concentrations despite the full tungsten coating of the inner wall and the addition of an impurity with high sputtering capability (Ar). The lower right figure inset shows time traces of a comparable discharge without ELM control, exhibiting radiative runaways with short H-L transitions.

In conclusion, maintaining of a minimum ELM frequency of 40 Hz enforced by small HFS pellet injection results in an integrated, fully controlled scenario with favorable divertor conditions which should also be applicable in a future full-tungsten ASDEX Upgrade tokamak.

References

[1] P.T. Lang et al., Nucl. Fusion **36** (1996) 1531.
[2] H. Zohm et al., "Overview of ASDEX Upgrade Results", IAEA FEC 2002, Lyon, Sept. 2002.
[3] P.T. Lang et al., Nucl. Fusion **41** (2001) 1107.
[4] A. Herrmann, Plasma Phys. Control. Fusion **44** 1 (2002).
[5] V. Mertens et al., Fusion Science and Technology in press.
[6] A. Kallenbach et al., J. Nucl. Mat. **290-293** (2001) 1184.